Socorro Air Quality Impacts from Regional Fires: A Case Study of 28 November 2018

Jaimy Karacaoglu, Christian M. Carrico

Department of Civil & Environmental Engineering

New Mexico Institute of Mining and Technology, Socorro, NM USA

Abstract

A short in duration but significant impact air quality event occurred on 28 November 2018 along the Rio Grande Valley of New Mexico. This occurred outside the spring to fall wildfire season, and greatly impacted air quality in Socorro, NM and the surrounding area for several hours that afternoon. Measurements of the air quality impact from the smoke event used a light scattering technique (integrating nephelometer) and a particulate mass concentration monitor (Dustrak optical monitor). Instruments were sampling ambient air during the event on the campus of New Mexico Institute of Mining and Technology in Socorro, New Mexico. Peak values of light scattering, and PM mass concentration reached 470 Mm⁻¹ and 0.28 mg/m³, respectively, on a 5-min basis. We examined the meteorological context of the event using local meteorological data and back-trajectories using the National Oceanic and Atmospheric Administration (NOAA) Hybrid Single Particle Lagrangian Integrated Trajectory (HYSPLIT) model to determine atmospheric transport and possible sources. Several fires, both prescribed and wildfires, occurred in the region including a prescribed burn at Bosque del Apache National Wildlife Refuge (20 km south-southeast of the receptor site) and a wildfire in Cibola County, NM (140 km northwest of the receptor site). Analysis of available data suggests that the prescribed burn at Bosque del Apache was the dominant contributor to the episode due to winds and the narrow spatiotemporal extent of the event. The increasing importance of restoring ecosystem function using prescribed fire in wildland fire management will likely lead to more frequent air quality impacts such as this and setup tradeoffs between these public goods.

1. Introduction

Smoke emitted by regional wildland fires has a significant and growing impact on air quality in the Western United States (Laing & Jaffe, 2019), including New Mexico with significant interplay with climate (Westerling et al., 2006). For decades, western U.S. wildfires, have increased in size and severity linked to changes in climate, such as longer, hotter summers (Abatzoglu & Williams, 2016), and increasing human activities, including both fire ignitions and fire suppression activities (Westerling et al., 2006). Aerosols from wildfires and prescribed fires contain both particulate matter and gas-phase pollutants (McMeeking et al., 2005). PM_{2.5} (particulate matter with a diameter less than 2.5 µm) penetrates deeply into human lungs causing substantial damage (Xing et al., 2016), and reduces atmospheric visibility by scattering and absorbing solar radiation (Malm, 1999). The latter effects also make PM_{2.5} relevant to regional climate changes (IPCC).

1.1 Wildfires and Biomass Smoke Emissions

Due to human activities such as fire ignitions and fire suppression activities as well as hotter and longer summers, wildfires have increased in both size and severity (Westerling et al., 2006). To mitigate this, various forest management techniques have been implemented, such as prescribed burns. Prescribed burns are meant to reduce fuel, restore woodlands, and manage landscapes according to the National Park Service. Prescribed burns, particularly regarding the reduction of hazardous fuel loads, play an integral part in reducing both the severity and size of wildfires in the future as well as reducing the risk of wildfires that could potentially affect nearby developed areas and ecosystems.

Though the number of wildfires in the United States has declined modestly in recent decades, the fire size and acreage burned with each fire have increased dramatically (www.nifc.gov). Gas phase species that are emitted through biomass burning include carbon monoxide (CO), carbon dioxide (CO₂) (~71% of emissions mass), nitrogen oxides (NO_x), and volatile organic compounds (VOCs) (Andreae & Merlet, 2001)(Liu et al., 2013). Particulate matter emitted includes both organic carbon and elemental carbon (Bond et al., 2013). Depending on the fuel combusted, significant primary emissions of inorganic ions may occur (McMeeking et al., 2009) (Gomez et al., 2018). The emissions of both trace gases and particulate matter can reduce the overall solar radiation that is absorbed by Earth's atmosphere during fire events. This can cause climate effects within the region of the event such as suppression of clouds and precipitation, enhancements of climate anomalies, and a reduction in surface temperature (Liu et al, 2013).

The overall intent of this case study is to diagnose the observed smoke on 28 November 2018 in the context of meteorology and sampled and surrounding aerosol properties. Regional data available for extinction composition, haze index, and wind speed and direction are examined. A comparison will be made to a previous occurrence within the region to draw comparisons on the effects a smoke event has on extinction composition and haze as well as visibility.

2. Methods

2.1 Sampling Site

All measurements were taken on 28 November 2018 at the New Mexico Institute of Mining and Technology campus in Socorro, New Mexico (located at 34.067° N 106.907° W at an elevation of 1,396 m ASL). Continuous ambient sampling was being conducted at this site which gave the opportunity to sample smoke events in real time with in-situ measurements. Figure 1 below shows the process flow diagram of the sampling site. One nephelometer (Ecotech Inc., M9003

520nm) and one Dusttrak Aerosol Monitor (TSI, Inc., Model 8520) were sampling outdoor air. The Dusttrak featured a $2.5~\mu m$ size cut at the inlet.

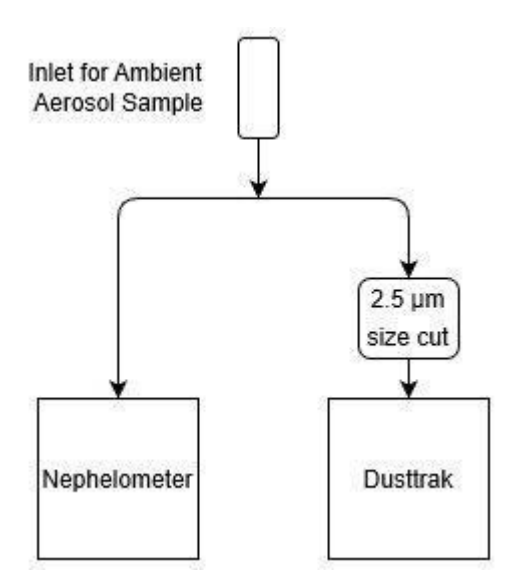


Figure 1: Process flow diagram of sampling site, including a nephelometer and a dusttrak sampling outdoor aerosol samples.

The closest meteorological data was being collected at a local Weather Station, located at 34.066 ° N 106.901 ° W and is less than 0.5 km from the sampling site.

2.2 Measurements

We report light scattering by particle coefficients (σ_{sp}), in Mm⁻¹, at a frequency of 5-minute averages with a 5 lpm flow rate with a single wavelength integrating nephelometer (Ecotech Inc., M9003 520 nm). Light scattering values are reported as measured and no corrections to STP or for truncation losses (measuring slightly less than the entire phase function) are applied. The mean instrument relative humidity (RH) over a 24-hour period was approximately 12.6% with a standard deviation of 1.6 which allows for any effects the RH may have had on the collected data to be deemed negligible. The light scattering coefficient was measured. To arrive at a total light extinction coefficient, soot light absorption, absorption by gases (dominated by NO₂) and

Rayleigh Scattering would need to be added to the measured light scattering coefficient. The instrument makes the following assumption to arrive at an approximate extinction coefficient:

$$\sigma_{\rm ext} \approx \sigma_{\rm scat} = \sigma_{\rm sg} + \sigma_{\rm sp}$$
 (1)

where σ_{ext} is the extinction coefficient, σ_{scat} is the scattering coefficient, σ_{sg} is the scattering due to gases and is also referred to as 'Rayleigh scattering', and σ_{sp} is the scattering due to particles.

Nephelometer Flow Diagram

Span Gas Room Air Sample Inlet **Raw Data** Aerosol Sample Flow Span Calibration Flow Sample Coarse Particulate-Free Air Calibration Flow Pump Filter Shared Calibration Flow Display Span Gas Zero Instrument Cell Valve Air Pump **Baffles** Measurement Zero Light **PMT** Volume Valve Trap Shutter Light Source **Filter**

Figure 2: Light path, aerosol sample path, and calibration paths inside of the single wavelength integrating nephelometer.

The nephelometer was calibrated using CO_2 as a span gas and HEPA-filtered air as a zero gas. The gases run through a set of two filters, one fine and one coarse, to eliminate all particles and measure σ_{sg} for which the value for CO_2 is known to be 34.87 Mm⁻¹ at STP (273.15 K, 1013.2 mBar). The nephelometer then uses the measured value, compared to this standard as well as the zero point and corrects the calibration curve accordingly. The nephelometer real-time measurements of temperature and pressure to calculate and subtract Rayleigh scattering (scattering by gases) from the measured value to give particulate light scattering coefficients.

Table 1: Nephelometer calibration data. The expected value for CO₂ was corrected for actual conditions in Socorro, NM (295K, 855mBar).

Type of Calibration	Expected Mean		Standard Deviation	Sample Size	
CO ₂ Calibration Gas	19.4 Mm ⁻¹	18.6 Mm ⁻¹	3.2	3	
Particulate Free Air	0.0 Mm ⁻¹	- 0.4 Mm ⁻¹	0.2	3	

We also measured particulate matter concentrations, in mg/m³, at a frequency of 5-minute averages with a flow rate of 1 lpm with a Dusttrak Aerosol Monitor (TSI, Inc., Model 8520). The instrument use fixed angle light scattering to yield an approximate mass concentration of particulate matter. A fixed angle 90° light scattering sensor is used, with a range of 0.001 to 100 mg/m³ and a zero stability of ± 0.001 mg/m³ over 24 hours using a 10-second time constant.. A temperature correction is applied at ± 0.001 mg/m³ per °C above the temperature at which the Dusttrak was zeroed. The Dusttrak operated with a factory calibration completed 6 months prior to sampling, and HEPA filter zero-adjustments (which removes 99.99% of particles from the gas stream) conducted both before and after the measurements were used to constrain uncertainties (PM2.5 changes < 0.001 mg/m³).

2.3 Visibility Calculations

To calculate visibility, or the distance an object can be clearly seen from, the Koschmeider relationship is used (Malm, 1999), which is defined as the following:

where L_v is the visibility range in km and σ_{ext} is the extinction coefficient in km⁻¹. It is used as an approximate method for calculating the visual range as a function of extinction coefficient (Malm, 1999). The visual range thus represents an upper bound on the true value.

Haze Index, measured in deciviews, is also used as a measure of visibility. It is considered a metric of haze proportional to the logarithm of the atmospheric extinction and is used to track compliance with the Regional Haze Rule according to the Interagency Monitoring of Protected Visual Environments (IMPROVE) and is calculated with Equation 3. For the calculations done for this event, the assumption that $\sigma_{ext} \approx \sigma_{sp}$ is used and we neglect any light absorption contribution. IMPROVE data presented within utilizes the haze index as a descriptor for visibility reduction. The haze index is a metric where a change in DV is approximately equivalent irrespective of the magnitude of light extinction.

$$D \diamondsuit \diamondsuit = \diamondsuit \diamondsuit \times \frac{1}{100} \diamondsuit \begin{bmatrix} \sigma_{e} \diamondsuit \diamondsuit t \end{bmatrix} \tag{3}$$

Table 2: Deciview values and their corresponding visibility levels as derived from the EPA's Introduction to Visibility Issues.

Deciviews	Light Extinction	Visibility Range	Qualitative Visibility
≤14	≤ 41 Mm ⁻¹	≥ 95 km	Very Good
15-20	41 Mm ⁻¹ – 74 Mm ⁻¹	53 km – 95 km	Good
21-24	74 Mm ⁻¹ – 110 Mm ⁻¹	36 km – 53 km	Moderate
25-28	110 Mm ⁻¹ – 164 Mm ⁻¹	24 km – 36 km	Bad
≥29	≥ 164 Mm ⁻¹	≤ 24 km	Very Bad

Table 2 provides insight into what deciviews indicate in regard to visibility and how it can be used to attribute conditions to air quality measurements. Listed also are the corresponding ranges of light extinction and visibility to allow for comparison between the three types of air quality descriptors. The EPA considers a visibility range of more than 95 km and a deciview value of less than 14 to be an indicator of very good air quality and little haziness. On the other end of the scale, the EPA considers a visibility range of less than 24 km and a deciview value greater than 29 to be an indicator of very bad air quality with a high level of haziness.

2.3 HYSPLIT Air Mass Back-Trajectory Modeling

The Hybrid Single-Particle Lagrangian Integrated Trajectory model (HYSPLIT), developed by the National Oceanic and Atmospheric Administration (NOAA), is a useful tool for backtrajectory modeling based on meteorological data (Stein et al., 2015).

The model simulated for this event was conducted through the Real-Time Environmental Applications and Display System (READY) (Ralph et al., 1993). HRRR meteorological data at 3 km resolution was used to run a backtrajectory, assuming isentropic vertical motion, originating at the sampling site beginning at 28 November 2018 at 2300 UTC (17:00 PM MDT). Atmospheric heights of 500m, 1000m, and 1500m above ground level were used with no midlayer boundary height. The backtrajectory traces back in time where the air masses arriving at the measurement site passed prior to arriving during the time of the smoke event.

3. Results and Discussions

The Nephelometer measured particulate light scattering coefficients ranged from ~0 to 470 Mm⁻¹ (5-min averages) as seen in Figure 3. From the measured values, visibility was calculated using the Koschmeider relationship (ignoring absorption terms). At background aerosol concentration and particle scattering coefficients close to 0 Mm⁻¹, the visual range was calculated to be 260 km (Rayleigh scattering only). At the peak of the episode, a greatly reduced visual range of 8.7 km was observed with a haze index of 38.5 deciviews.

With the dusttrak, measured particulate concentration ranged from ~ 0 to 0.28 mg/m³ as seen in Figure 3. The 24-hr PM_{2.5} National Ambient Air Quality standard, eight times lower than the peak concentration observed, is also indicated at 35 μ g/m³ for reference of severity. Even with

the short nature of the event, the 24-hr $PM_{2.5}$ concentration on 28 November 2018 was 26.6 $\mu g/m^3$.

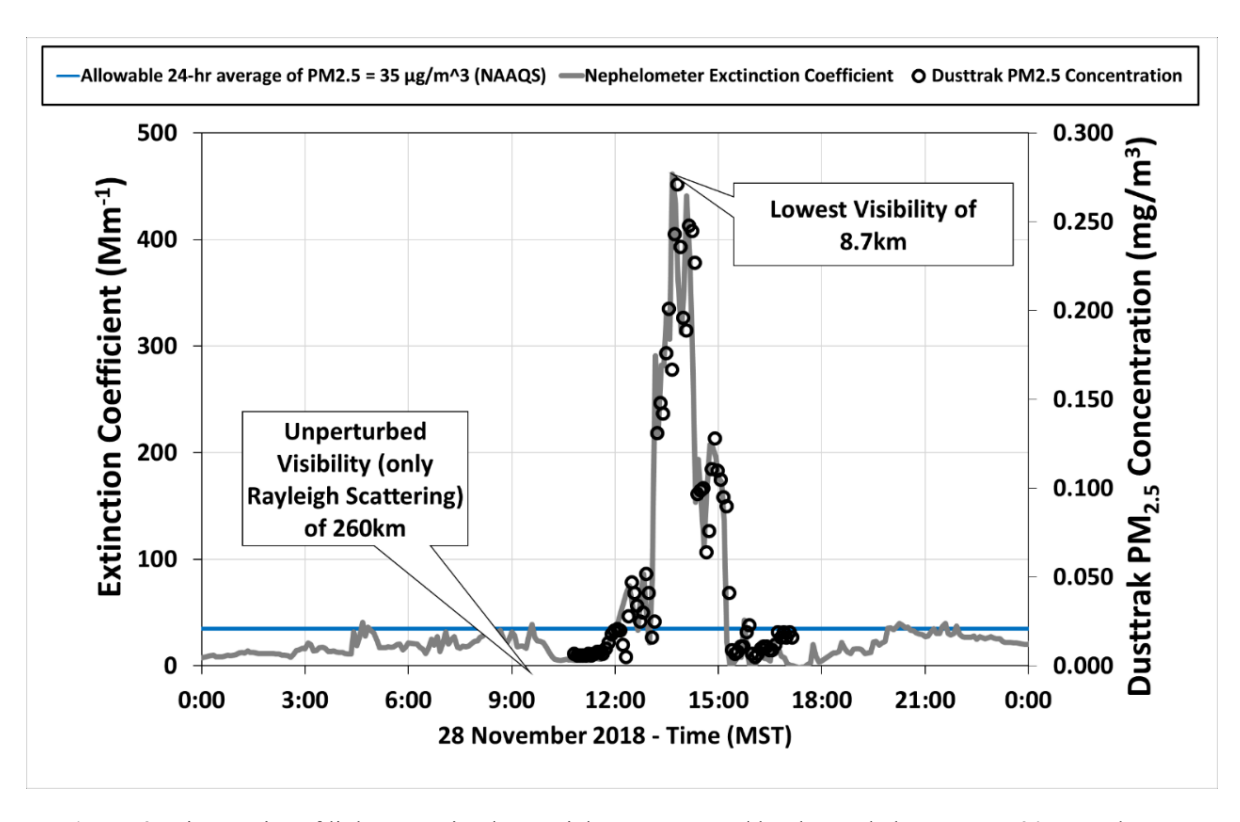


Figure 3: Time series of light scattering by particles as measured by the nephelometer at 520nm and PM_{2.5} concentration as measured by the Dusttrak. Estimated visual ranges are indicated at 'natural' visibility (Rayleigh scattering only) and lowest visual range which occurred during the peak of the event. The blue line indicates the 24-hour National Ambient Air Quality Standards as listed under 40 CFR part 50.

With both the nephelometer and dusttrak data collected, a mass scattering efficiency can be graphically calculated as seen in Figure 4. The two instruments tracked very closely during the event as indicated by the high $R^2 = 0.97$. By taking the slope from this regression, a mass scattering efficiency of 1.70 m²/g is retrieved. This value may show a higher concentration of course mode particles, such as soot, present during this episode (Hand & Malm, 2007). With a typical range of 2 m²/g to 6 m²/g for scattering efficiency, the calculated value of 1.70 m²/g indicates a very fresh smoke aerosol with small particles that have not yet grown to sizes efficient at light scattering.

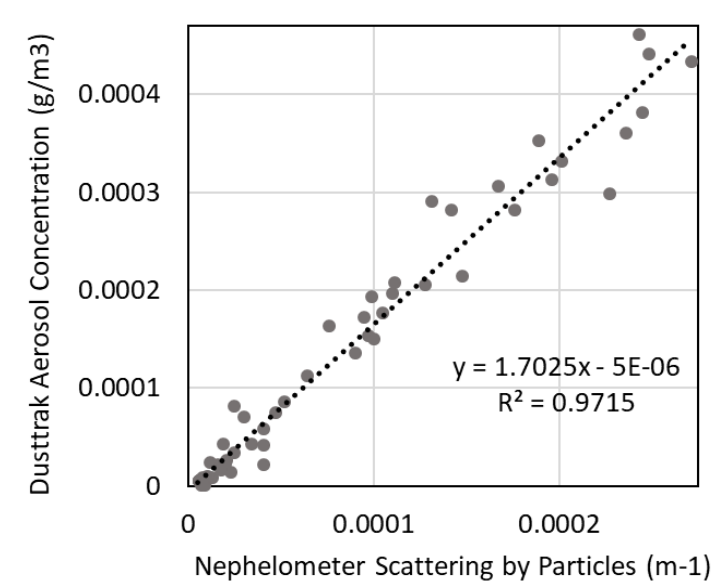


Figure 4: Mass Scattering Efficiency in g/m² is retrieved from the slope of the regression.

A summary of the PM_{2.5} chemical composition from 28 November 2018 the local Bosque del Apache IMPROVE monitoring station is shown in Figure 5. The apportionment of light extinction based on composition analysis of 24-hour filter samples using IMPROVE algorithms for the apportionment of light extinction. The dominance of elemental and organic carbon is typical of ambient sampled biomass smoke aerosols (McMeeking et al., 2005).

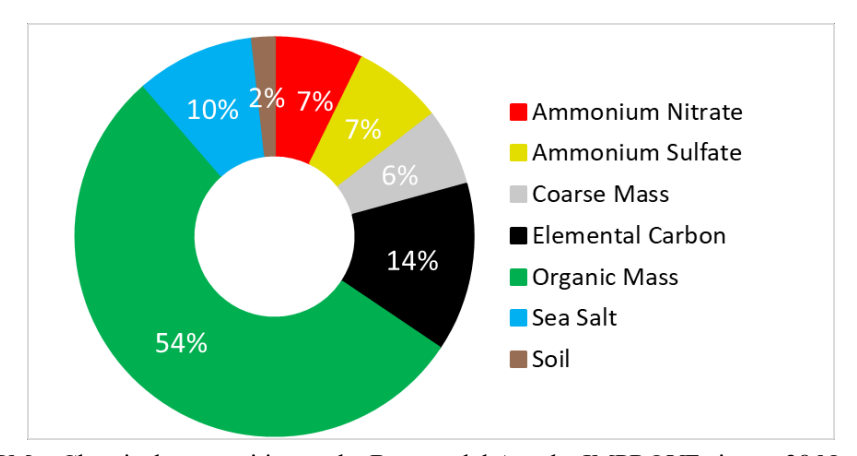


Figure 5: PM_{2.5} Chemical composition at the Bosque del Apache IMPROVE site on 28 November 2018.

Using a NOAA HYSPLIT model to run backtrajectory analysis, as seen in Figure 6, a clear direction of mesoscale atmospheric transport can be mapped. Two fires known to have been actively burning and producing smoke at the time are also indicated on the map.

The model features six trajectories, each representing different air parcels as they move from their initial position, at two hour intervals from a starting heigh of 500 m AGL. The red and yellow trajectories would both be considered fast moving air parcels as they cover a large distance in the modeled 24 hours. The dark blue trajectory shows a relatively similar path of motion as both the red and the yellow trajectories, with all three coming from the west where no significant smoke events were occuring at the time. The red and the green trajectories show an intersection between the atmospheric transport backtrajectory and the location of the Bosque del Apache fire. The green trajectory is a clear indicator that the prescibed fire at Bosque del Apache may be the main component that attributed to the smoke event due the circular nature of the air parcel it models. The light blue and pink trajectories show relatively the same behavior as the green trajectory with a circular motion of the air parcel around the Socorro, New Mexico region.

NOAA HYSPLIT MODEL Backward trajectories ending at 2300 UTC 28 Nov 18 HRRR Meteorological Data

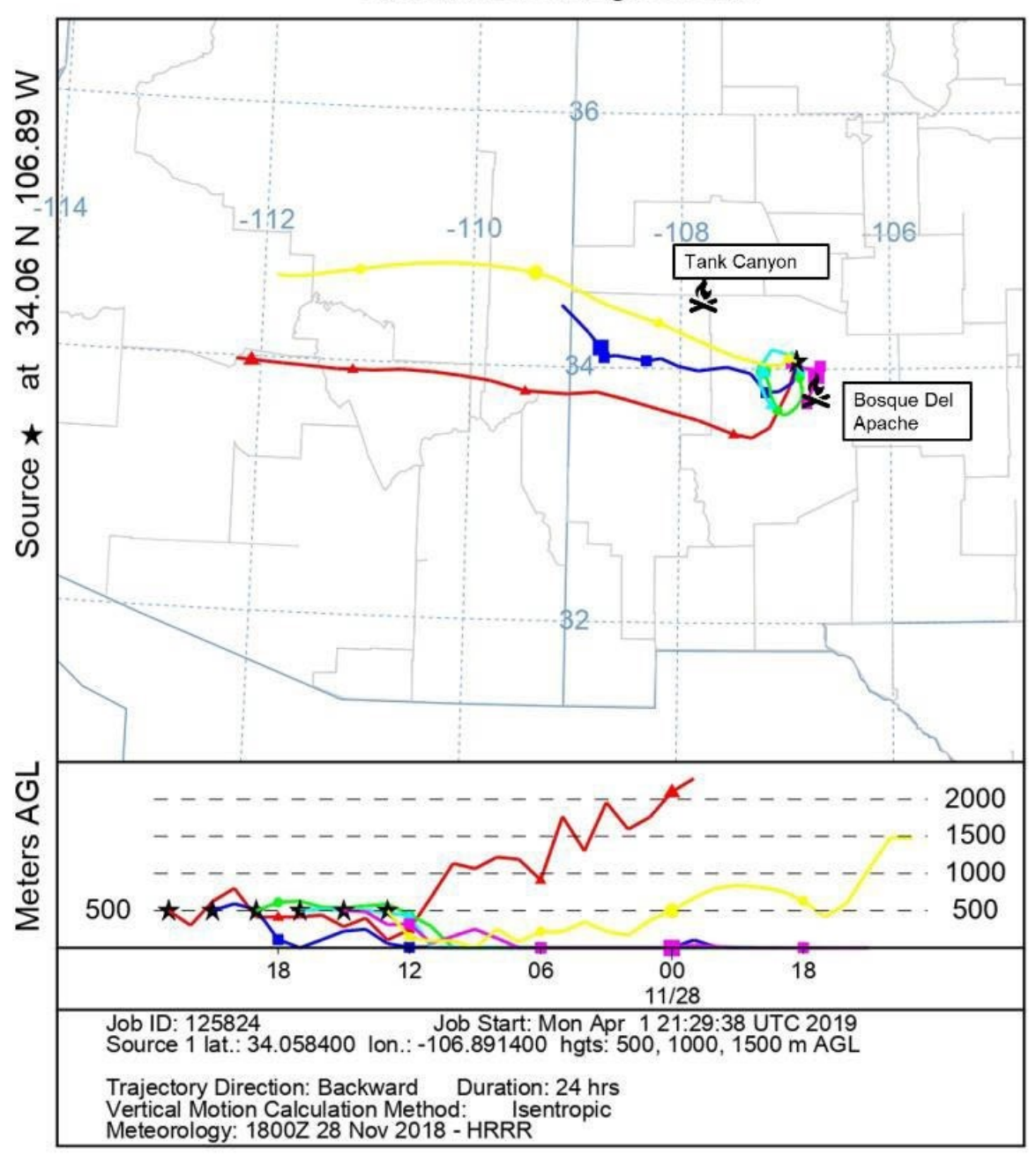


Figure 6: HYSPLIT Model conducted beginning on 2300 UTC. Two known fires are indicated on the map.

A map-based version of the model is depicted in Figure 7 to provide clearer indication of the location of the Bosque Del Apache National Wildlife Refuge and the Northern Cibola National Forest. There is no clear intersection with the Northern Cibola National Forest, where the Tank Canyon Fire occurred, and any of the trajectories. It can be seen, however, that there is a clear intersection between multiple air parcel trajectories and the Bosque del Apache that also intersect with Socorro, New Mexico. This shows that air parcels that had been located at and around the Bosque Del Apache were transported to the Socorro, New Mexico region. This is further supported with wind speed and direction data collected from the Socorro Municipal Airport discussed next.

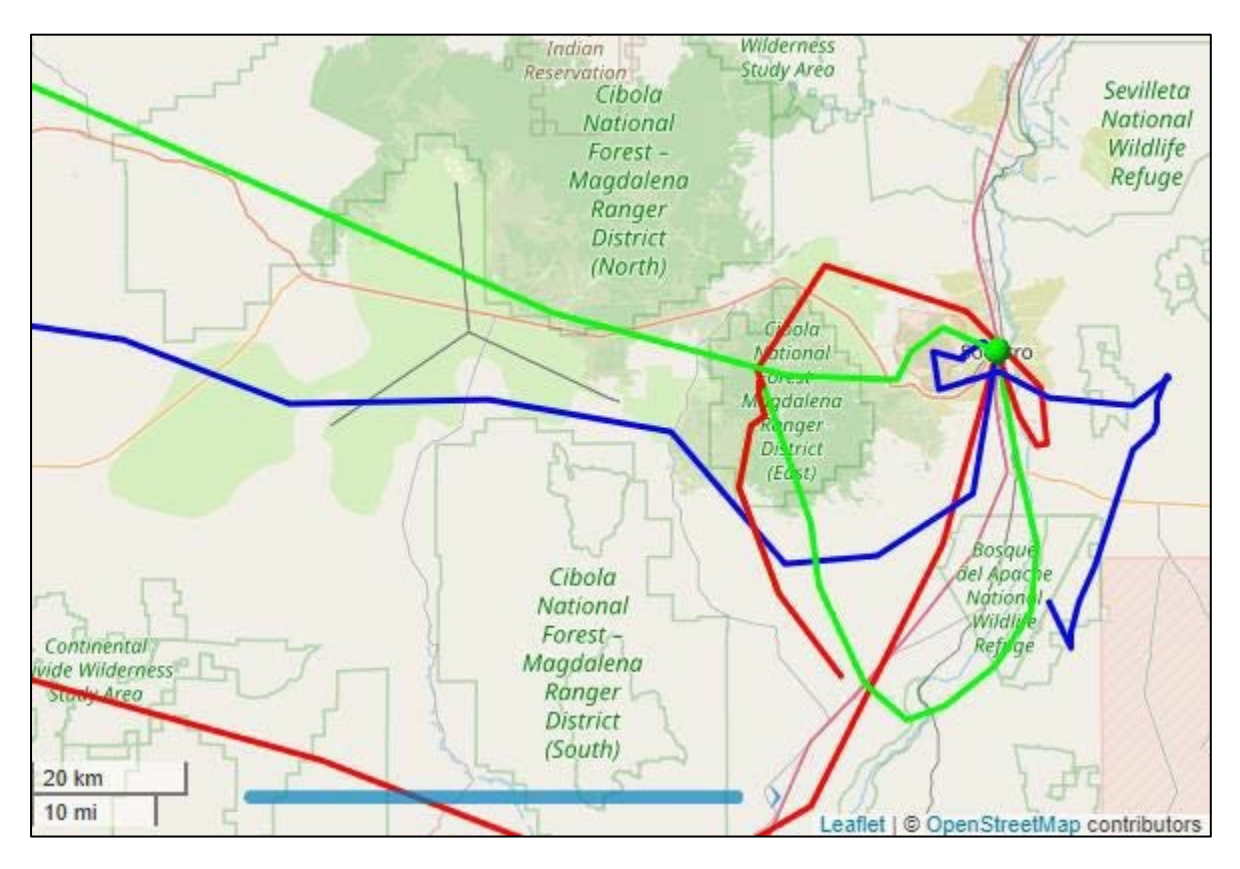


Figure 7: Regional map view with overlay of model lines. Base map and data from OpenStreetMap and OpenStreetMap Foundation.

The local wind data for the 28 November 2018 is shown in Figure 7 and Figure 8. During the hours of the haze event in Socorro, local winds shifted to south-southeast beginning late morning

and lasting until approximately 6pm local time. Elevated PM_{2.5} concentrations follow the wind pattern quite closely also showing the local nature of the event was likely confined to the Rio Grande Valley where day-night upriver-downriver atmospheric flow occurs.

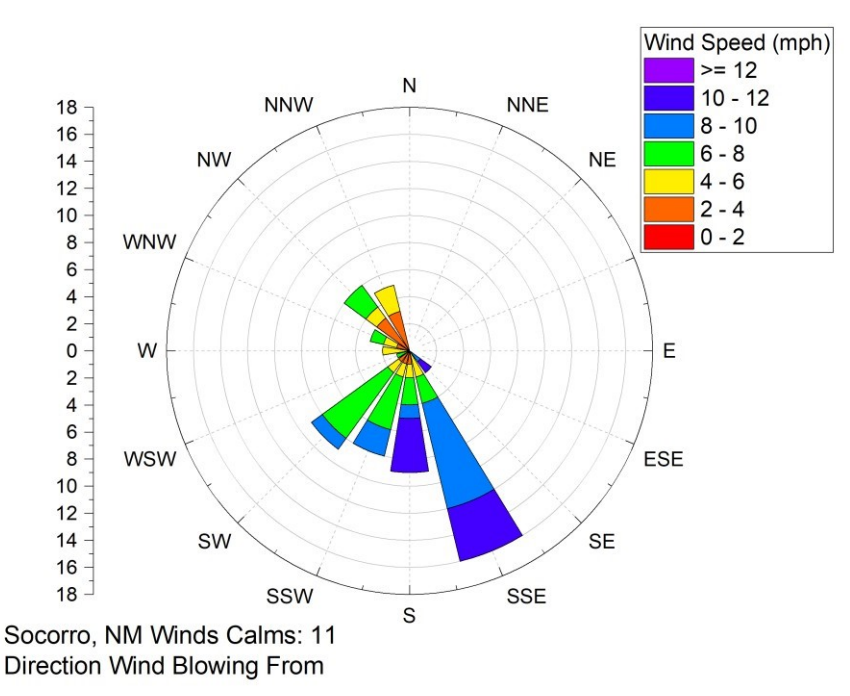


Figure 7: Local Socorro, New Mexico wind speed and direction data plotted as a wind rose.

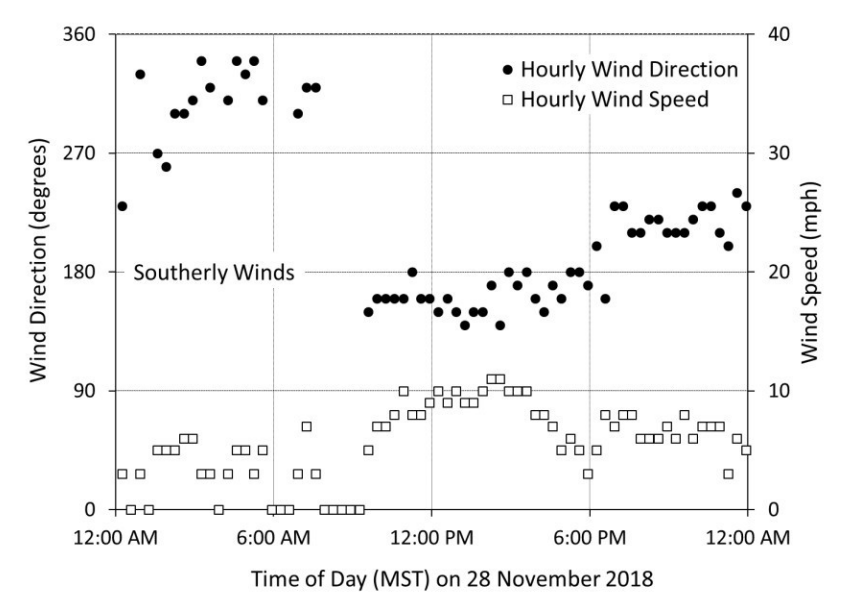


Figure 8: Local Socorro, New Mexico wind speed and direction plot on 28 November 2018.

The Interagency Monitoring Network for Protected Visual Environments (IMPROVE) is a nationwide network of remote sites for monitoring regional aerosol properties in scenic areas

including national parks and monuments (Malm, 1999). We examined data from nearby IMPROVE network monitoring stations in New Mexico and Arizona during this suspected smoke event. Regional stations' data records examined included 6 sites in NM, 4 in Arizona, and 4 in Colorado. The nearest station is Bosque del Apache (BOAP1) which is near San Antonio, NM and is approximately 17 km south of the Socorro site. BOAP1 and Socorro are both located in the Rio Grande Valley, extending from north to south from the Rocky Mountains of southern Colorado to the border with Mexico on the south.

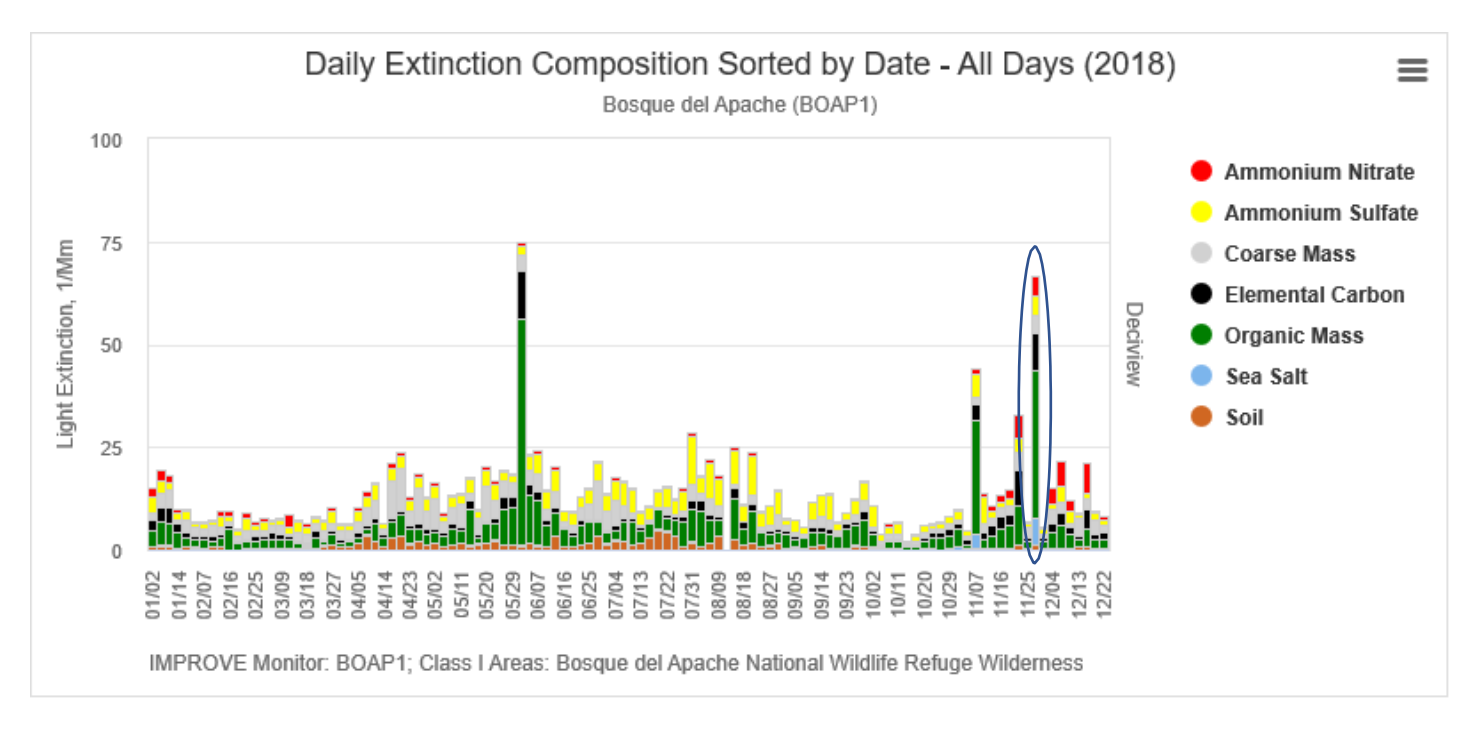


Figure 9: Bosque del Apache (BOAP1) daily extinction composition in 1/Mm t in 2018. 28 November 2018 Smoke event day is indicated. Data from IMPROVE monitoring network output from the Western Regional Air Partnership Technical Support System (https://views.cira.colostate.edu/tssv2/)

The surrounding IMPROVE monitoring sites were examined for the same sampling day of 28 November 2018 to assess a regional impact of the event. The measured haze metric, the IMPROVE attributed anthropogenic component, and the remaining natural component (this includes biomass burning) is given in Table 3 (all given in the haze metric deciviews, dV). IMPROVE sites in New Mexico as well as bordering sites in Arizona and Colorado are included,

totaling 15 monitoring sites. As is often the case in winter, visibility is typically background conditions of ~5 deciviews. Bosque del Apache is the lone site that shows elevated haziness with most of this attributed to natural sources as shown in Table 3. Evidence from surrounding sites shows they are under good visibility conditions and the smoke here is likely driven from more proximate sources.

Table 3: IMPROVE site data for 28 November 2018. NA= Data Not Available.

Class 1 Area	IMPROVE monitor	Visibility condition (deciviews)	Anthropogenic Impairment (deciviews)	Natural Sources (deciviews)
Bandelier Wilderness	BAND1	4.6	2.0	2.6
Bosque del Apache Wilderness	BOAP1	20.4	1.9	18.5
Carlsbad Caverns National Park	GUMO1	12.2	6.4	5.8
Gila Wilderness	GICL1	3.2	1.7	1.5
Salt Creek Wilderness	SACR1	7.9	5.1	2.8
San Pedro Parks Wilderness	SAPE1	0.5	0.9	<0>
Wheeler Peak Wilderness	WHPE1	NA	NA	NA
White Mountain Wilderness	WHIT1	3.7	2.0	1.7
Petrified Forest National Park (AZ)	PEFO1	5.2	2.4	2.8
Mount Baldy (AZ)	BALD1	0.8	0.8	0
Chiricahua (AZ)	CHIR1	5.1	2.0	3.1
Grand Canyon National Park (AZ)	GRCA2	4.2	1.7	2.5
Shamrock Mine (CO)	SHMI1	3.5	2.0	1.5
Mesa Verde National Park (CO)	MESA1	2.8	1.1	1.7
Weminuche Wilderness (CO)	WEMI1	2.9	1.5	1.4
Great Sand Dunes National Monument (CO)	GRSA1	3.1	1.7	1.4

No other nearby stations showed a significant perturbation above the typically observed background concentrations. At BOAP1, the event on 28 November 2018 was the second largest concentration measured during the year. The reconstructed 24-hour $PM_{2.5}$ mass concentration was approximately 50 $\mu g/m^3$ and the composition was dominated by organic carbon with a secondary contribution from elemental carbon as typical with ambient smoke events (McMeeking et al., 2005) (Figure 10). The reconstructed 24-hour light extinction coefficient

was approximately 70 Mm⁻¹ during this event. IMPROVE algorithms attributed the majority of haze to natural sources which includes biomass burning smoke (Figure 10). Comparing to Socorro 24-hour light extinction of 42 Mm⁻¹, it was of similar magnitude. The confinement of the event to the Rio Grande valley gives evidence that it was more likely the local prescribed fire occurring that day rather than a regional scale event.

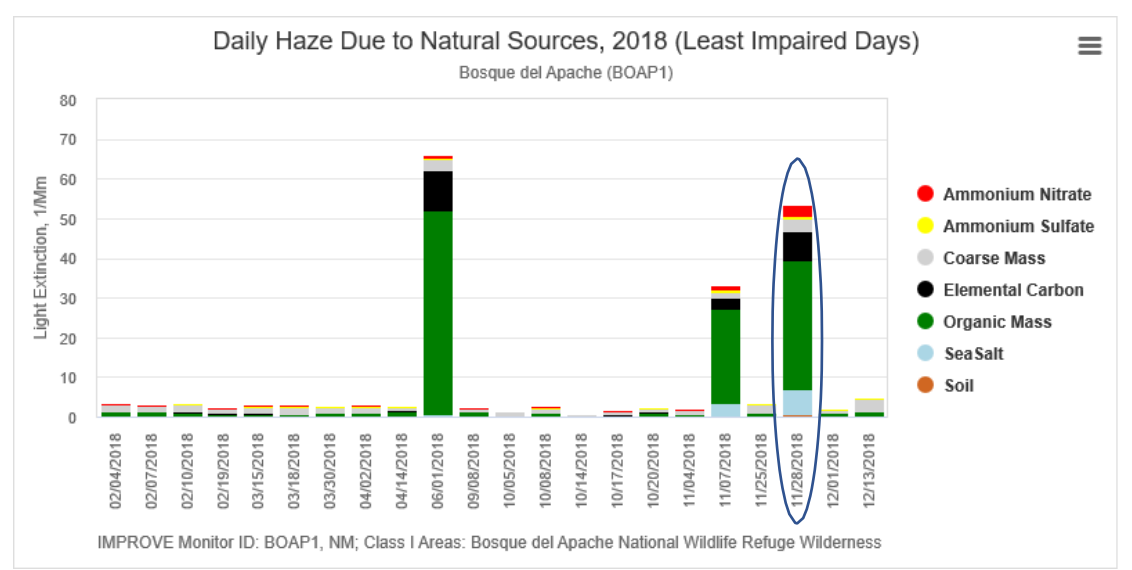


Figure 10: Daily Haze Due to Natural Sources in 2018 and its composition as measured in light extinction, Mm⁻¹.

For comparison, Figure 11 below depicts the same infographics for the year 2012 to illustrate the effects of a regional scale smoke event. The Whitewater-Baldy Complex Fire, the largest recorded wildfire event in New Mexico history, started on 9 May 2012 and by 4 June 2012 it had burned approximately 241,000 acres of coniferous forest. A large increase in daily extinction to about 300 Mm⁻¹ is also seen during this period as seen in Figure 11 with a similar composition with what is seen during the 28 November 2018 incident. The haze index was also severely increased to approximately 34 deciviews during this time period. This is indicative of severe visibility reduction in the area at the time of the event. Effects from the event though persisted for approximately 2 weeks and over multiple days as seen in the data in Figure 11. Like the

incident examined here, most of the haze was attributed to natural sources (i.e. biomass burning) and consisted of a dominant organic and elemental carbon composition.

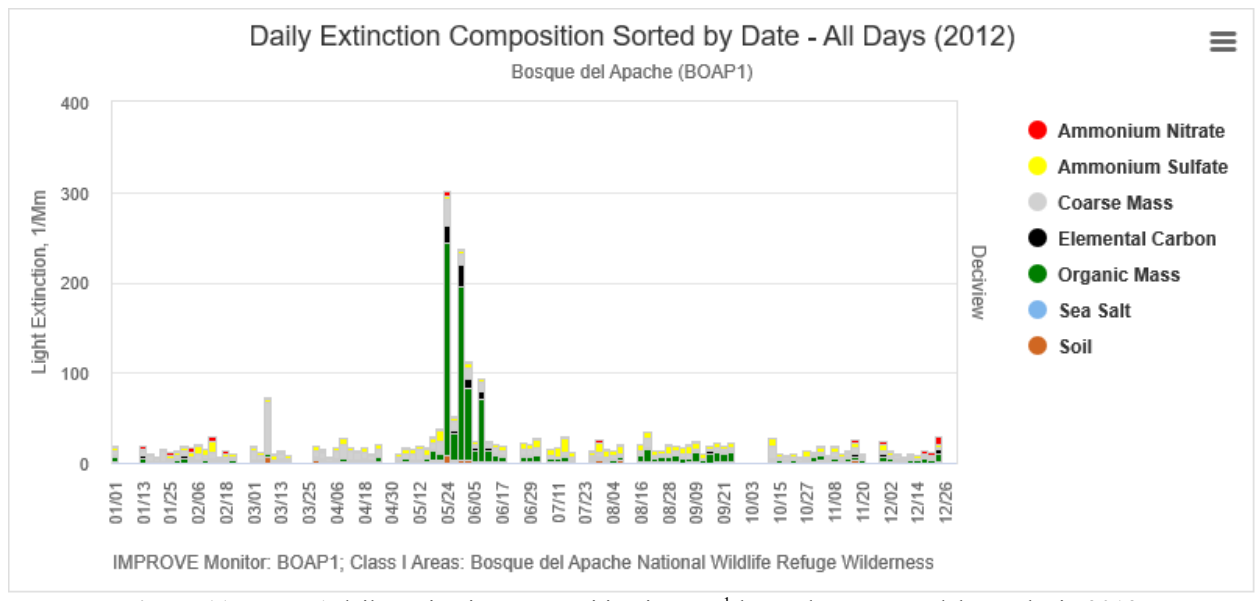


Figure 11: BOAP1 daily extinction composition in Mm⁻¹ located at Bosque del Apache in 2012.

4. Conclusions

An extreme in magnitude though short in time frame haze event with severely degraded air quality occurred in Socorro, NM on the afternoon of 28 November 2018. With the data presented herein, it can be concluded that the origins of the haze on the afternoon of 28 November 2018 was driven primarily by smoke from a prescribed burn located at the Bosque del Apache near San Antonio, New Mexico. The smoke caused a significant reduction in visibility, with a haze index of 38.5 deciviews and an extinction coefficient (5-min average) maximum of 470 Mm⁻¹. This equates to a minimum in visual range of 8.7 km. Local wind data, paired with backtrajectory analysis using the NOAA HYSPLIT Model, suggest transport from this more proximate fire dominated over the Tank Canyon Fire in Cibola County, New Mexico. Further inquiry into the Bosque del Apache wildlife refuge prescribed burn showed that this event produced more significant smoke than anticipated from the burning and smoldering of salt cedar

on the refuge. Comparisons to another incident in mid-2012 during the Whitewater-Baldy fire showed similar featured in aerosol composition, visibility, and haze index, though the earlier event was of longer magnitude and more regional in nature. The increasing use of prescribed burning, a vital tool for ecosystem management and to mitigate wildfire frequency and severity, will likely lead to more conflicts between the former goals and maintaining air quality.

5. Acknowledgements

This work was supported in part by the U.S. National Science Foundation.

The authors gratefully acknowledge the NOAA Air Resources Laboratory (ARL) for the provision of the HYSPLIT transport and dispersion model and/or READY website (https://www.ready.noaa.gov) used in this publication.

The authors gratefully acknowledge OpenStreetMap and its contributors for the provision of the OpenStreetMap base map and associated data licensed under the OpenDataCommonsOpen

DatabaseLicense (ODbL) by the OpenStreetMapFoundation (OSMF).

IMPROVE is a collaborative association of state, tribal, and federal agencies, and international partners. US Environmental Protection Agency is the primary funding source, with contracting and research support from the National Park Service. The Air Quality Group at the University of California, Davis is the central analytical laboratory, with ion analysis provided by Research Triangle Institute, and carbon analysis provided by Desert Research Institute.

The authors also acknowledge Dr. Carrico's Fall 2018 Air Resources Engineering students who aided in the collection of the data presented herein.

References

- Abatzoglou, J. T., & A. P. Williams (2016). Impact of anthropogenic climate change on wildfire across western US forests. *P. Natl. Acad. Sci. USA* 113 (42):11770-11775. doi: 10.1073/pnas.1607171113.
- Andreae, M. O., & Merlet, P. (2001), Emission of trace gases and aerosols from biomass burning, *Global Biogeochem. Cycles*, 15(4), 955–966, doi:10.1029/2000GB001382.
- Bond, T. C., Doherty, S.J., Fahey, D.W., Forster, P. M., Bernsten, T., DeAngelo, B. J., Flanner, M.G., Ghan, S., Kärcher, B., Koch, D., Kinne, S., Kondo, Y., Quinn, P.K., Sarofim, M.C., Schultz, M.G., Schulz, M., Venkataraman, C., Zhang, H., Zhang, S., ...Zender, C. S. (2013), Bounding the role of black carbon in the climate system: A scientific assessment, *J. Geophys. Res. Atmos.*, 118, 5380–5552, doi:10.1002/jgrd.50171.
- Carrico, C. M., Gomez, S. L., Dubey, M. K., & Aiken, A. C. (2018). Low hygroscopicity of ambient fresh carbonaceous aerosols from pyrotechnics smoke. Atmospheric Environment, 178, 101–108. doi: 10.1016/j.atmosenv.2018.01.024.
- Gomez, S. L., Carrico, C. M., Allen, C., Lam, J., Dabli, S., Sullivan, A. P., Aiken, A. C., Rahn, T., Romonosky, D., Chylek, P., Sevanto, S., & Dubey, M.K. (2018), Southwestern U.S. biomass burning smoke hygroscopicity: the role of plant phenology, chemical composition, and combustion properties. *J. Geophys. Res.-Atmos.* 123 (10):5416-5432. doi: 10.1029/2017JD028162.
- Hand, J. L., & Malm, W. C. (2007). Review of aerosol mass scattering efficiencies from ground-based measurements since 1990. Journal of Geophysical Research, 112(D16). doi: 10.1029/2007jd008484.
- Laing, J.R. & Jaffe, D.A. (2019). Wildfires are causing extreme PM concentrations in the western United States. *EM* July 2019.
- Levin, E. J. T., McMeeking, G.R., Carrico, C. M., Mack, L.E., Kreidenweis, S. M., Wold, C. E., Moosmüller, H., Arnott, W. P., Hao, W. M., Collett, J. L., Malm, W. C., (2010), Biomass burning smoke aerosol properties measured during Fire Laboratory at Missoula Experiments (FLAME), *J. Geophys. Res.*, 115, D18210, doi:10.1029/2009JD013601.
- Li, L., Chen, C., Fu, J. S., Huang, C., Streets, D. G., Huang, H. Y., Zhang, G. F., Wang, Y. J., Jang, C. J., Wang, H. L., Chen, Y. R., & Fu, J. M., (2011). Air quality and emissions in the Yangtze River Delta, China. *Atmospheric Chemistry and Physics*. 10. doi: 10.5194/acpd-10-23657-2010.
- Liu, Y., Goodrick, S., & Heilman, W. (2013). Wildland fire emissions, carbon, and climate: Wildfire–climate interactions. *Forest ecology and management, 317*, 80-96. doi: 10.1016/j.foreco.2013.02.020
- Malm, W. C. (1999). Introduction to Visibility, 1–70. doi: 10.1016/b978-0-12-804450-6.00001-2

- M9003 Nephelometer Operations Manual. (n.d.) (Vol. 1).
- McMeeking, G. R., Kreidenweis, S. M., Carrico, C. M., Collett, J. L., Day, D. E., & Malm, W. C., (2005), Observations of smoke-influenced aerosol during the Yosemite Aerosol Characterization Study: 2. Aerosol scattering and absorbing properties, *J. Geophys. Res.*, 110, D18209, doi:10.1029/2004JD005624.
- McMeeking, G. R., Kredenweis, S. M., Baker, S., Carrico, C. M., Chow, J. C., Collett Jr., J. L., Hao, W. M., Holden, A. S., Kirchstetter, T. W., Malm, W. C., Moosmüller, H., Sullivan, A. P., & Wold, C. E. (2009), Emissions of trace gases and aerosols during the open combustion of biomass in the laboratory, *J. Geophys. Res.*, 114, D19210, doi:10.1029/2009JD011836.
- Model 8520 DusttrakTM Aerosol Monitor, (2010).
- Rolph, G., Stein, A., & Stunder, B., (2017). Real-time Environmental Applications and Display System: READY. Environmental Modelling & Software, **95**, 210-228, doi: 10.1016/j.envsoft.2017.06.025
- Stein, A.F., Draxler, R.R, Rolph, G.D., Stunder, B.J.B., Cohen, M.D., & Ngan, F., (2015). NOAA's HYSPLIT atmospheric transport and dispersion modeling system, Bull. Amer. Meteor. Soc., **96**, 2059-2077, doi: 10.1175/BAMS-D-14-00110.1
- Westerling, A. L., Hidalgo, H.G. Cayan, D.R., & Swetnam, T.W., (2006). Warming and Earlier Spring Increase Western U.S. Forest Wildfire Activity. Science, 313 (5789), 940–943. doi: 10.1126/science.1128834
- Xing, Y. F., Xu, Y. H., Shi, M. H., & Lian, Y. X. (2016). The impact of PM2.5 on the human respiratory system. *Journal of thoracic disease*, 8(1), E69–E74. doi: 10.3978/j.issn.2072-1439.2016.01.19